RESEARCH PAPER

Quality-by-Design Optimisation of Talazoparib-Loaded Lipid–Polymer Hybrid Nanoparticles Using a Box–Behnken Design: Preparation, Characterisation, *In-Vitro* Release and Cytotoxicity in MDA-MB-231 Cells

Jayaprakash K[1], Kamaleshwari. B[1]*, Dr.R.Gayathri[1], Cathrien J[1], Kalaimani A[1], Gnana Infant Josuva S[1],Jeelani B[2], Balakrishnan B[3], Anton D divine[4], Farisha P[4]

[1] Department of Pharmaceutics, KMCH College of Pharmacy, Coimbatore, Affiliated to The Tamil Nadu Dr. M.G.R. Medical University, Chennai.

[2] Department of Pharmaceutics, Vinayaka Mission's College of Pharmacy, Vinayaka Mission Research foundation(Deemed to be University), Salem.

[3] Department of Physics, P.T.Lee Chengalvaraya Naicker College of Engineering & Technology, Kancheepuram

[4]Department of Pharmaceutics, United College of Pharmacy, Coimbatore, Affiliated to The Tamil Nadu Dr. M.G.R. Medical University, Chennai.

* Corresponding author: Mrs.B.Kamaleshwari

Email: b.kamali22@gmail.com

Received: 20th June 2026; **Revised:** 29th July 2026; **Accepted:** 15th October 2026; **Available Online:** 17th October 2026

Abstract

Talazoparib is a highly potent PARP-trapping agent shown to be effective in the treatment of triple negative breast cancer with mutations in the BRCA genes, although its poorly aqueous solubility and haematological toxicity are two factors that restrict its use. We aimed to develop Talazoparib-loaded lipid–polymer hybrid nanoparticles (L-PNPs) and optimise them by quality by design (QbD). L-PNPs were prepared from using the nanoprecipitation method of Corbion PURASORB® PDLG 5002A, soya lecithin and Poloxamer 188. The Box–Behnken design (15 runs) with three factors and three levels was used to evaluate particle size, polydispersity index (PDI) and entrapment efficiency (EE) of the particle size production. Dynamic Light scattering, Zeta Potential, SEM, FTIR, drug content and in vitro release (dialysis bag method and Phosphate buffered saline pH 7.4) along with MTT-assay performed on MDA-MB-231 cells were used for characterisation of the optimised formulation (R17). No new peak appearance or shift were found by FTIR, which would suggest any chemical interaction. The particlesize was significantly affected by the amount of polymer (PDLG) ($p = 0.0005$) and PDI and EE were significantly created impact by the amount of lipid ($p = 0.0055$ and 0.0058, respectively). R17 (PDLG 30.00 mg, lecithin 29.56 mg, Poloxamer 188 50.00 mg) had a Z-average size of 127.3 nm, PDI 0.379, zeta potential −21.3 mV, EE 89.75 % and drug content 96.25 %. Experimental values differed from predictions by −22.3 % (size), −27.0 % (PDI) and −8.0 % (EE). Release dose from 7.5 % at 1 h to 87.0 % at 8 h, and was best described by the Korsmeyer–Peppas model ($R^2 = 0.9514$, $n = 1.285$). After 24 h, IC_{50} values were 2.870 µM for R17 and 8.456 µM for free Talazoparib. A Talazoparib L-PNP with a particle size of approximately 130 nm and good entrapment was acquired. The optimisation models were almost predictive and there was no drug-free carrier control, so additional research is required before the lower IC_{50} can be alone credited to the delivery of nanoparticles.

Keywords: Talazoparib; lipid–polymer hybrid nanoparticles; quality by design; Box–Behnken design; triple-negative breast cancer; PARP inhibitor/trapping, MDA-MB-231

How to cite this article: Jayaprakash K. Quality-by-Design Optimisation of Talazoparib-Loaded Lipid–Polymer Hybrid Nanoparticles Using a Box–Behnken Design: Preparation, Characterisation, In-Vitro Release and Cytotoxicity in MDA-MB-231 Cells. Int J Drug Deliv Technol. 2026;16(88s):1985-1993. DOI: 10.25258/ijddt.16.88s.203.

1. Introduction

Triple-negative breast cancer (TNBC) lacks expression of the oestrogen receptor, progesterone receptor and HER2. It accounts for about 10–20 % of breast cancers and has an aggressive course, so endocrine and HER2-directed therapies are not effective.[1]

Chemotherapy with anthracyclines, taxanes and platinum agents remains the challenge of treatment, and a pathological complete response after neoadjuvant therapy is associated with better long-term survival.[2] Adding the immune checkpoint inhibitor pembrolizumab to chemotherapy improved survival in early-stage disease,[2] and the antibody–drug conjugate Sacituzumab govitecan improved outcomes in metastatic disease.[3] These options are limited by systemic toxicity, resistance and cost, and targeted therapy is therefore needed.

For patients with germline BRCA1/2 mutations, poly(ADP-ribose) polymerase (PARP) inhibitors exploit a defect in homologous-recombination repair. Olaparib was effective in the OlympiAD trial,[4] and Talazoparib (BMN 673) is a highly potent PARP1/2 inhibitor[5] and, among the approved PARP inhibitors, the most potent at trapping PARP on DNA;[6] it prolonged progression-free survival compared with standard chemotherapy in the EMBRACA trial (median 8.6 vs 5.6 months).[7,8]

The clinical use of Talazoparib is nevertheless limited by dose-related haematological toxicity,[6] and, as shown here, by its very low aqueous solubility. Encapsulation in a nanocarrier could improve the apparent solubility and change the exposure of the drug, and nanoparticles can accumulate in tumours through the enhanced

permeability and retention effect.[9] Two Talazoparib nanoformulations have been reported, a nanoemulsion for parenteral use and Talazoparib nanoparticles for overcoming multidrug resistance in TNBC cells.[10,11]

Lipid–polymer hybrid nanoparticles (L-PNPs) combine a biodegradable polymeric core, which holds the drug and sustained release, with a phospholipid layer that improves biocompatibility and stability.[12–14] Hybrid systems of this kind have been optimised for several drugs.[15–18] Quality by design (QbD), as described in ICH Q8(R2), links formulation variables to critical quality attributes through designed experiments and is increasingly applied to nanomedicines.[19–21] To our knowledge, a QbD-optimised PDLG–lecithin hybrid nanoparticle of Talazoparib has not been described.

The aim of this study was to prepare Talazoparib-loaded L-PNPs from PDLG 5002A, soya lecithin and Poloxamer 188, optimise the polymer, lipid and stabiliser amounts with a Box–Behnken design, and characterise the optimised formulation, including drug release and cytotoxicity in MDA-MB-231 cells.

2. Materials and methods

2.1 Materials

Talazoparib (catalogue BD305506, lot HKA347; HPLC purity 99.99 % by supplier certificate) was obtained from BLD Pharmatech (India) Pvt Ltd. Corbion PURASORB® PDLG 5002A (50:50 DL-lactide/glycolide; inherent viscosity 0.20 dl/g; acid number 9.6 mg KOH/g; batch 7500587301) was supplied by Corbion (PURAC Biochem BV). Soya lecithin powder (97 %) was from Otto Chemie Pvt Ltd. Poloxamer 188, dimethyl sulfoxide (DMSO) and absolute ethanol were supplied by the Department of Pharmaceutics, KMCH College of Pharma; Milli-Q water was used. MDA-MB-231 cells, DMEM, fetal bovine serum (FBS) and MTT were used for cell studies.

2.2 Pre-formulation studies

Appearance was recorded visually. Qualitative solubility was assessed in water, aqueous buffers, ethanol, DMSO and dimethylformamide using the pharmacopoeial descriptive terms. The melting point was measured by the capillary method (Labholic LH-108). For UV quantification, stock solutions in DMSO were diluted with ethanol to 2–20 µg/mL, absorbance was read at 310 nm (Shimadzu UV-1800, 1 cm quartz cell) and a linear calibration was fitted including the blank (0, 0) point; LOD and LOQ were estimated as 1.07 and 3.25 µg/mL. Drug–excipient compatibility was examined by FTIR (JASCO FT/IR-4100 with an ATR PRO ONE accessory; 4000–400 cm^{-1}; scanning speed auto, 2 mm/s;) for Talazoparib, PDLG 5002A, soya lecithin, Poloxamer 188, a physical mixture in the proportions of the optimised formulation (about 2.7 % w/w drug) and the freeze-dried optimised formulation.[22]

2.3 Preparation of L-PNPs

L-PNPs were prepared by nanoprecipitation. Talazoparib (3 mg), PDLG 5002A and soya lecithin were dissolved in 3 mL of DMSO–ethanol (2:1, v/v). This organic phase was added at 1 mL/min to 20 mL of Milli-Q water containing Poloxamer 188 under stirring at 1000 rpm at room temperature. The dispersion was probe-sonicated at 40 % amplitude for 3 min (5 s pulses on/off) in an ice bath and stirred to evaporate ethanol. Nanoparticles were separated by centrifugation at 5000 rpm (about 2236 × g) for 5 min at 4 °C, washed with Milli-Q water to remove DMSO and unentrapped material, and redispersed in Milli-Q water. The sonication amplitude (30, 40 and 50 %) was screened in preliminary trials.

2.4 Experimental design and optimisation

A three-factor, three-level Box–Behnken design (15 runs with three centre points) was generated with Design-Expert® 13.[23] The factors were the amounts of PDLG 5002A (X_1, 10–30 mg), soya lecithin (X_2, 10–40 mg) and Poloxamer 188 (X_3, 50–100 mg) (Table 1). The responses were particle size (Y_1), PDI (Y_2) and EE (Y_3). Quadratic models were fitted and assessed by ANOVA, R^2, adjusted and predicted R^2, adequate precision and lack of fit. Numerical optimisation sought minimum size, minimum PDI and maximum EE using the desirability function. The optimum was prepared and the experimental responses were compared with predictions: prediction error (%) = (experimental − predicted) / predicted × 100.

2.5 Characterisation of the optimised formulation

Z-average size, PDI and zeta potential were measured by dynamic light scattering and electrophoretic light scattering (HORIBA SZ-100V2) after dilution in Milli-Q water at [25 °C] [n = 3]. Morphology was examined by SEM (TESCAN MIRA3, 15 kV) after drying and conductive coating. For drug content, 1 mL of dispersion was dissolved in DMSO, diluted with DMSO–ethanol and read at 310 nm. EE was determined indirectly from free drug in the supernatant after centrifugation: EE (%) = (total drug − free drug) / total drug × 100. Drug loading (DL) was defined as entrapped drug / (entrapped drug + carrier mass) × 100.

2.6 *In vitro* release

Release was studied by dialysis (membrane MWCO 12–14 kDa) against 25 mL phosphate-buffered saline (pH 7.4), after placing 1 mL of the R17 dispersion in the dialysis bag at 37 ± 0.5 °C and 50 rpm. Samples (1 mL) were withdrawn at 1, 2, 3, 4, 5, 6 and 8 h and replaced with fresh medium. Samples were diluted 10-fold with DMSO–ethanol and read at 310 nm against a calibration prepared in the same medium. Cumulative release was corrected for withdrawn volume: $Q_n = V \cdot C_n + Vs \cdot \Sigma C_i$. Data were fitted to zero-order, first-order, Higuchi and Korsmeyer–Peppas models.[24,25]

2.7 Cytotoxicity

The MTT assay was performed at the BioMe laboratory, Karaikudi. MDA-MB-231 cells were cultured in DMEM with 10 % FBS at 37 °C in 5 % CO_2 and seeded at 5 × 10^3 cells/well in 96-well plates. After overnight attachment, cells were treated for 24 h with free Talazoparib or R17 L-PNPs at 0.01, 0.03, 0.1, 0.3, 1, 3, 10 and 30 µM (Talazoparib equivalent); final DMSO was ≤ 0.1 % (v/v). MTT (5 mg/mL) was added for 3–4 h, formazan was dissolved in 200 µL DMSO and absorbance read at 570 nm. Viability was expressed relative to untreated cells. IC_{50} values and 95 % confidence intervals were obtained by variable-slope non-linear regression in GraphPad Prism 11. A drug-free L-PNP control was not included.

3. Results and discussion

3.1 Pre-formulation and drug–excipient compatibility

Talazoparib was a white to off-white, fine, free-flowing powder. It was practically insoluble in water, sparingly soluble in aqueous buffers, slightly soluble in ethanol and freely soluble in DMSO and DMF, which supported the DMSO–ethanol organic phase. The melting point was 257.1 °C, within the reference range of 257–259 °C. The UV calibration at 310 nm was linear over 0–20 µg/mL ($y = 0.0092x + 0.0008$, $R^2 = 0.9986$; blank point included), with an LOD of 1.07 µg/mL and an LOQ of 3.25 µg/mL.

FTIR spectra are compared in Figure 1. The ester C=O band of PDLG 5002A (1739.48 cm^{-1}) and soya lecithin (1737.55 cm^{-1}) was retained in the physical mixture (1738.51 cm^{-1}) and in the formulation (1736.58 cm^{-1}), a shift of about 3 cm^{-1} that is within the 4 cm^{-1} resolution. The P188 bands near 960 and 840 cm^{-1} remained in the physical mixture. The weak Talazoparib bands (for example 1659.45, 1600.63 and 1234.22 cm^{-1}) were not resolved in the mixture or the formulation because the drug is only about 2.7 % w/w and its bands overlap with excipient bands. The formulation showed a broad O–H/N–H band at about 3325 cm^{-1}, probably from P188 hydroxyl groups, hydrated lecithin and adsorbed water, and the aliphatic C–H stretching bands were not resolved. No new peak appeared. Therefore, FTIR showed no evidence of chemical interaction, but at this drug fraction it cannot exclude weak interactions, and DSC or XRD would be needed to establish the physical state of the drug.

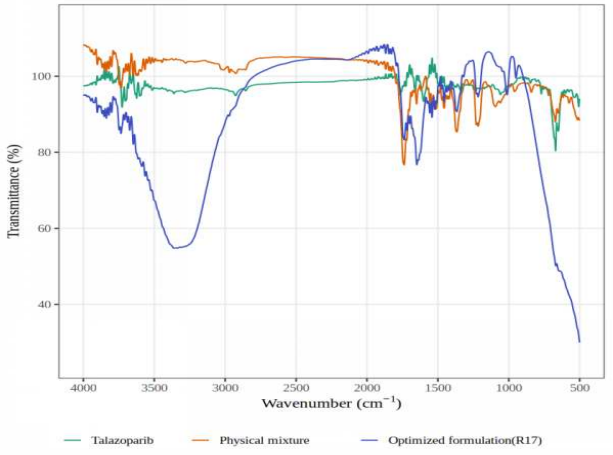


Figure 1 Overlay of the FTIR spectra of Talazoparib, the physical mixture and the optimized formulation (R17 L-PNPs) on a common transmittance scale.

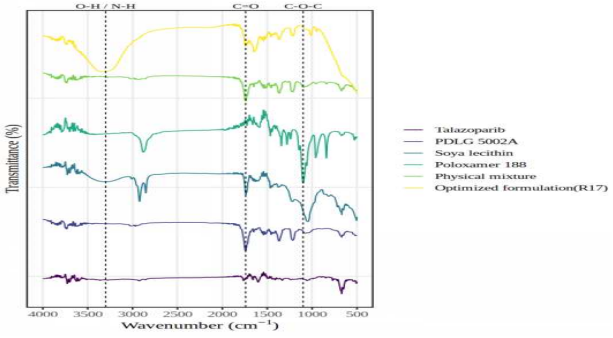


Figure 2.Stacked FTIR spectra (recorded 4000–400 cm^{-1}) of soya lecithin, Poloxamer 188 (P188), PDLG 5002A, Talazoparib, the Talazoparib–excipient physical mixture and the optimised formulation (TLZ-LPNs, R17). Spectra are vertically offset; dashed lines mark O–H/N–H (~3330 cm^{-1}), C=O (~1740 cm^{-1}) and C–O–C (~1100 cm^{-1}) regions.

3.2 Preliminary trials

Sonication amplitude created impact on particle size. At 30 % the mean particle size was 1895.37 ± 2617.84 nm (aggregates), at 40 % it was 247.17 ± 33.91 nm (PDI 0.377) and at 50 % it was 558.03 ± 322.22 nm. A confirmation run at 40 % gave 404.07 ± 300.27 nm, so repeatability at this setting was limited. Forty per cent was selected for the design.

3.3 Box–Behnken design

Table 1. Factors, levels and fixed conditions of the Box–Behnken design.

Factor	Low (−1)	Centre (0)	High (+1)
X_1 PDLG 5002A (mg)	10	20	30
X_2 Soya lecithin (mg)	10	25	40
X_3 Poloxamer 188 (mg)	50	75	100
Fixed per batch	Talazoparib 3 mg	DMSO–ethanol 2:1, 3 mL	Water 20 mL

Other fixed conditions: injection rate 1 mL/min, stirring 1000 rpm, room temperature, probe sonication at 40 % amplitude for 3 min and pulse 5 seconds on/off.

Table 2. Design matrix and observed responses (run order as performed).

Run	PDLG (mg)	Lecithin (mg)	P188 (mg)	Size (nm)	PDI	EE (%)
1	10	40	75	234.9	0.3897	87.3
2	20	40	50	166.6	0.3607	85.6
3	20	40	100	235.6	0.5327	82.3
4	30	40	75	620.83	0.4207	89.8
5	20	10	100	165.87	1.0327	95.6
6	20	25	75	247.17	0.3767	82.3
7	10	25	100	2185.77	2.9957	97.3
8	20	25	75	379.73	0.4587	94
9	20	10	50	1151.67	4.223	98.16

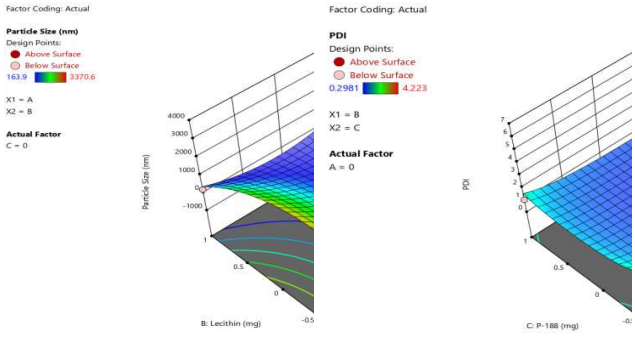
Run	PDLG (mg)	Lecithin (mg)	P188 (mg)	Size (nm)	PDI	EE (%)
10	30	25	50	190.7	0.3853	99
11	30	10	75	470.1	2.261	99.8
12	30	25	100	225.07	0.514	93.16
13	20	25	75	163.9	0.2981	81.6
14	10	25	50	3370.6	2.642	99
15	10	10	75	2634	1.6357	96.5

Particle size ranged from 163.9 to 3370.6 nm and EE from 81.6 to 99.8 %. In six runs (5, 7, 9, 11, 14 and 15) the PDI exceeded 1, and four of them gave sizes above 1 µm. PDI values above 1 indicate highly polydisperse or aggregated samples for which cumulant analysis is unreliable, so these runs did not give nanoparticles; they were kept in the model with caution. The three centre points differed considerably (163.9–379.7 nm; EE 81.6–94.0 %), which shows poor repeatability and inflates pure error.

Table 3. Model statistics for the three responses.

Statistic	Particle size	PDI	EE
Model p-value	0.0040	0.0375	0.0343
Lack of fit p-value	0.0938	0.2455	0.9894
R^2	0.9833	0.8099	0.8154
Adjusted R^2	0.9417	0.6198	0.6307
Predicted R^2	0.3929	0.2211	0.4611
Adequate precision	15.39	5.79	5.80

A **B**



C

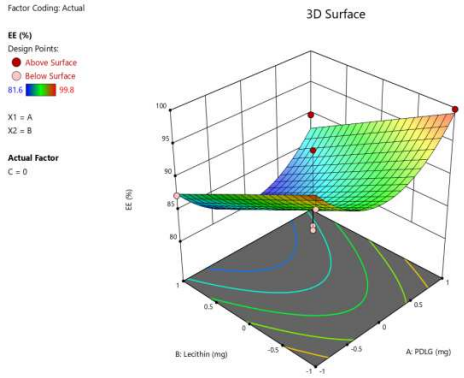


Figure 3 Three-dimensional response surface plots showing the effect of formulation variables on (A) particle size and (B) PDI AND (C) EEof Talazoparib-loaded hybrid lipid–polymer nanoparticles.

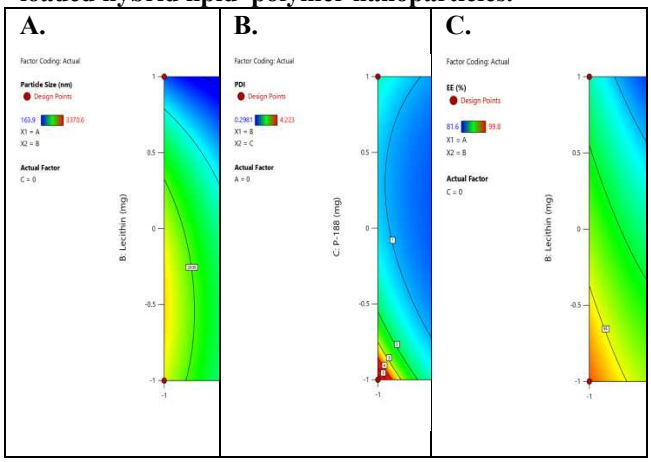


Figure 4 Contour plots showing the effect of formulation variables on (A) particle size, (B) polydispersity index (PDI), and (C) entrapment efficiency (EE) of Talazoparib-loaded hybrid lipid–polymer nanoparticles.

All three models were significant. PDLG amount had the largest effect on particle size ($p = 0.0005$), followed by lecithin ($p = 0.0112$), Poloxamer 188 ($p = 0.0438$), the PDLG × lecithin interaction ($p = 0.0071$) and the quadratic PDLG term ($p = 0.0024$). Lecithin was the only significant linear factor for PDI ($p = 0.0055$) and EE ($p = 0.0058$), and the quadratic PDLG term also influenced EE ($p = 0.0127$). A larger polymer content changes the viscosity of the organic phase and the nucleation and growth of particles during nanoprecipitation, which is consistent with the dominant effect of PDLG on size. The models must be read with caution: the predicted R^2 values are far below the adjusted R^2 (a gap greater than 0.2), the particle-size model has ten terms for 15 runs (four residual degrees of freedom), and the PDI model has a high coefficient of variation because of the aggregated runs. They are therefore used as a guide to the design space rather than as precise predictors.

3.4 Optimisation and validation

Numerical optimisation (desirability 0.861) gave PDLG 30.00 mg, soya lecithin 29.56 mg and Poloxamer 188 50.00 mg, with predicted size 163.9 nm, PDI 0.519 and

EE 97.5 %. Two factors lay at the edge of the design space (PDLG at +1 and Poloxamer 188 at −1), so the optimum may lie outside the region studied. The formulation was prepared as R17 (Table 4). The experimental size and PDI were lower than predicted (−22.3 % and −27.0 %), i.e. better than predicted, whereas EE was 8.0 % lower; only EE fell within 10 % of its prediction. This agrees with the low predicted R^2 values and shows that the validation was only partly successful.

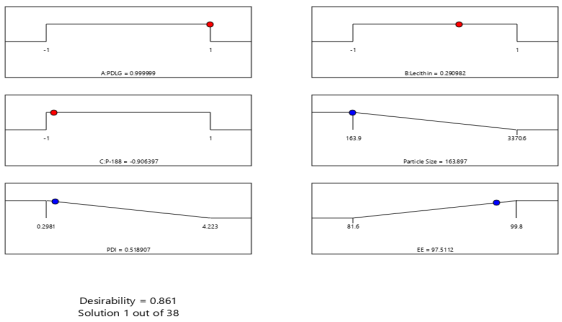


Figure 5 Desirability ramp plot showing the optimized levels of formulation variables and corresponding predicted responses.

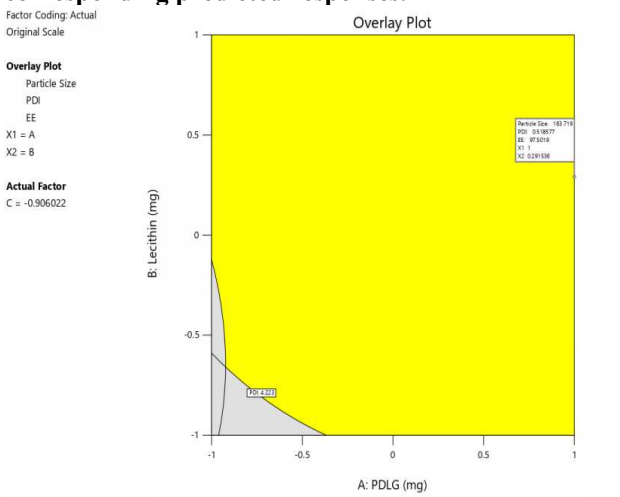


Figure 6 Optimization overlay plot showing the overall desirability and predicted responses for particle size, PDI, and entrapment efficiency at the selected formulation-variable levels.

Table 4. Predicted and experimental responses of R17.

Response	Predicted	Experimental	Prediction error (%)
Particle size (nm)	163.9	127.3	−22.33
PDI	0.519	0.379	−26.97
EE (%)	97.5	89.75	−7.96

3.5 Characterisation of R17

R17 had a Z-average of 127.3 nm and a PDI of 0.379, which indicates a moderate size distribution (a PDI below 0.3 is usually preferred). The zeta potential was −21.3 mV, which gives moderate electrostaticstabilisation. SEM showed predominantly spherical particles; the four particles measured were 54.37–93.69 nm (mean 73.21 nm) (indicative only). The smaller SEM size isexpected because SEM measures dried particles and DLS measures the hydrodynamic diameter. Drug content was 96.25 %, EE 89.75 % and DL 2.40 % (Table 5).

Figure 7 Scanning electron micrograph of optimized Talazoparib-loaded lipid–polymer hybrid nanoparticles (R17) showing spherical morphology and representative particle-size measurements.

Table 5. Content of talazoparib in talazoparib-filled lipid–polymer nanoparticles (L-PNPs) from 15 formulation batches.

Batch	Drug content (%)	Drug Loading (%)
1	97.71	2.05
2	94.37	2.28
3	98.54	1.52
4	96.87	1.82
5	91.04	2.16
6	99.79	2.02
7	97.71	2.12
8	97.92	2.30
9	91.25	3.55
10	94.58	2.75
11	93.75	2.54
12	99.17	1.77
13	96.46	2.00
14	98.12	3.38
15	94.37	2.96

Table 6. Characteristics of the optimised formulation R17.

Parameter	Value
Z-average size (nm)	127.3
PDI	0.379
Zeta potential (mV)	−21.3
SEM size (nm; n = 4)	73.21 (54.37–93.69)
Drug content (%)	96.25
Entrapment efficiency (%)	89.75

Parameter	Value
Drug loading (%)	2.40

The free-drug reading used for EE (absorbance 0.0131, about 1.34 µg/mL after dilution) lies above the LOD (1.07 µg/mL) but below the LOQ (3.25 µg/mL) and below the lowest calibration standard (2 µg/mL), so the EE value carries more uncertainty than the others.

3.6 *In-Vitro* release

Cumulative release increased from 7.47 % at 1 h to 15.64, 20.29, 32.57, 52.68 and 80.51 % at 2–6 h and 86.96 % at 8 h (Figure 2). The profile shows a slow start rather than a burst. Zero-order, first-order, Higuchi and Korsmeyer–Peppas models gave R^2 of 0.9273, 0.8306, 0.7202 and 0.9514 (adjusted R^2 0.9433), respectively. The Korsmeyer–Peppas exponent was n = 1.285, above the 0.85 limit for spheres,[25] which suggests release controlled by polymer relaxation or erosion (super case-II type). This is indicative only, because the model applies to roughly the first 60 % of release, only five points fall in that range and the dialysis membrane adds a lag. Because the study lasted only 8 h and the first three readings (about 0.8–2.1 µg/mL) are below the LOQ of 3.25 µg/mL, sustained release has not been demonstrate; Sink conditions in 25 mL PBS were not demonstrated, no free-drug dialysis control was run, and longer release studies are needed. Similar progressive release has been reported for other hybrid systems.[16,26]

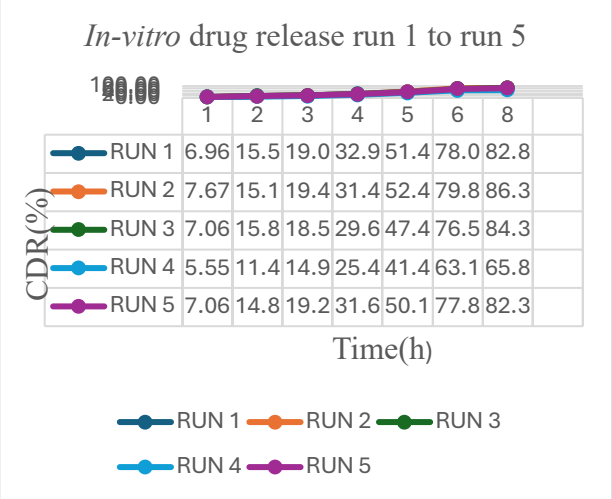


Figure 8. Comparative *In-Vitro* cumulative drug release profiles of Talazoparib-loaded L-PNPs formulations (Runs 1–5) over 8 hours.

Figure 9. Comparative *in vitro* cumulative drug release profiles of Talazoparib-loaded L-PNPsformulations (Runs 6–10) over 8 hours.

Figure 10. Comparative *in vitro* cumulative drug release profiles of Talazoparib-loaded L-PNPs formulations (Runs 11–15) over 8 hours.

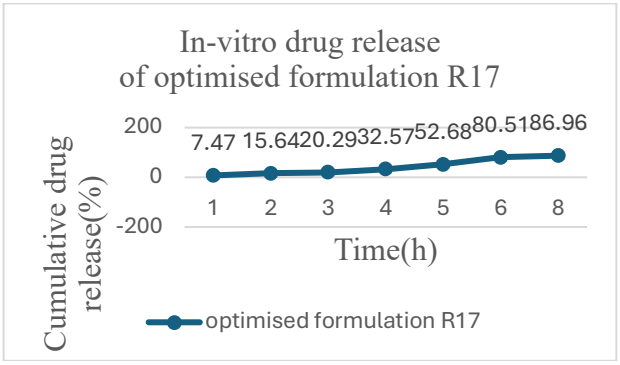


Figure11. Cumulative release of Talazoparib from R17 in PBS (pH 7.4, 37 °C).

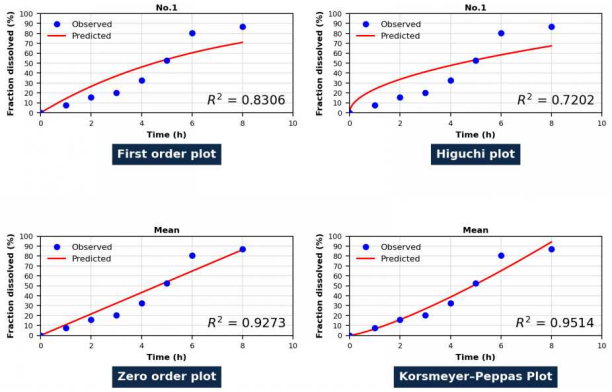


Figure 12. Kinetic modelling of the *in vitro* release of Talazoparib from the optimised formulation (R17 L-PNPs) in PBS (pH 7.4, 37 °C): first-order (R^2 = 0.8306), Higuchi (R^2 = 0.7202), zero-order (R^2 = 0.9273) and Korsmeyer–Peppas (R^2 = 0.9514) models. Blue circles are the observed cumulative release (%) and red lines are the model predictions.

3.7*In-Vitro* Cytotoxicity

Both samples reduced MDA-MB-231 viability in a concentration-dependent manner over 24 h (Figure 13). The IC_{50} was 8.456 µM (95 % CI 8.146–8.781; R^2 0.9987) for free Talazoparib and 2.870 µM (2.555–3.228; R^2 0.9906) for R17, a 2.95-fold (66.1 %) reduction. The free-drug IC_{50} is higher than the 0.45 µM reported for MDA-MB-231 in a cell-line panel,[27] which may reflect the short 24 h exposure, since PARP inhibitors usually act over longer periods, and the BRCA-proficient status of this cell line.[27,28]The lower IC_{50} of R17 cannot be attributed to nanoparticle delivery alone: no drug-free L-PNP control was included, so the contribution of lecithin, PDLG, Poloxamer 188 and residual DMSO to toxicity is unknown, and no statistical comparison of the two curves was made. Uptake, apoptosis and DNA-damage studies would be needed to explain the mechanism

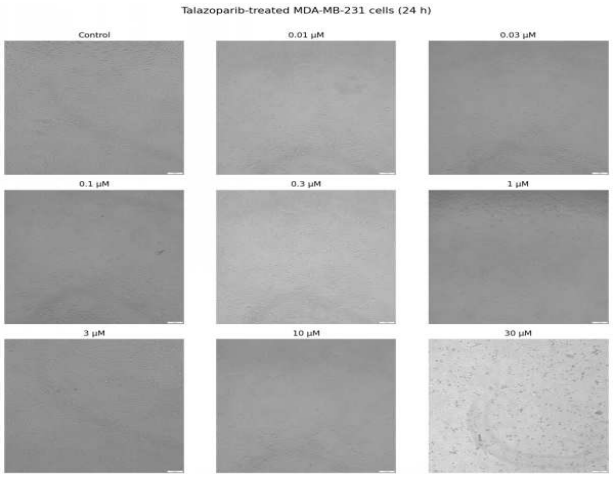


Figure 13Representative bright-field microscopic images of MDA-MB-231 triple-negative breast cancer cells following 24-hour treatment with talazoparib at concentrations of 0.01, 0.03, 0.1, 0.3, 1, 10, 3 & 30 µM, compared with the untreated control.

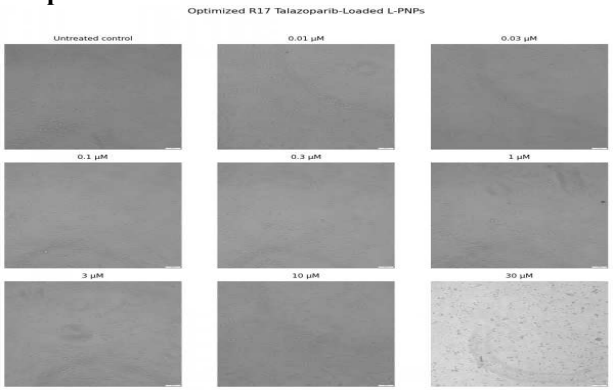


Figure 14. Representative bright-field microscopic images of MDA-MB-231 triple-negative breast cancer cells following 24-hour treatment with the optimized talazoparib-loaded lipid–polymer nanoparticle formulation (R17 L-PNPs) at equivalent talazoparib concentrations of 0.01, 0.03, 0.1, 0.3, 1, 3, 10, and 30 µM, compared with the untreated control.

Table 7. Cell viability (%) of MDA-MB-231 cells after 24 h, as reported in the thesis (singlevalues).

Concentration (µM)	Free Talazoparib	R17 L-PNPs
0.01	97	98
0.03	96	96
0.1	94	93
0.3	89	83
1	81	66
3	66	46
10	48	28
30	29	24

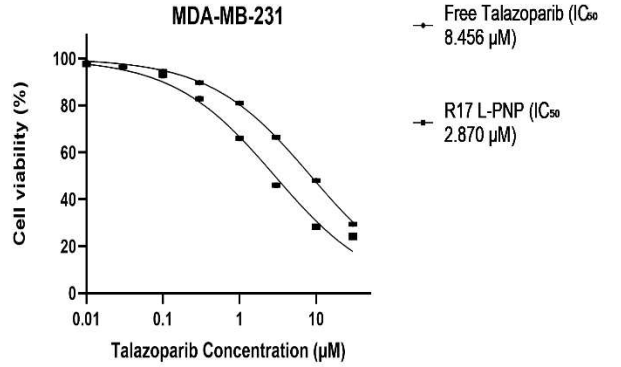


Figure 15. Viability of MDA-MB-231 cells after 24 h with free Talazoparib or R17 L-PNPs (MTT assay). Values are as reported in the thesis; the lines are variable-slope fits.

4. Summary

- Talazoparib-loaded lipid–polymer hybrid nanoparticles were made by nanoprecipitation.
- A Box–Behnken design linked polymer, lipid and stabiliser amounts to Particle size, PDI and entrapment.
- The optimised formulation: 127.3 nm, PDI 0.379, zeta potential −21.3 mV, entrapment 89.75 %.
- Release reached 86.96 % at 8 h; the Korsmeyer–Peppas model fitted best.
- IC_{50} in MDA-MB-231 cells was 2.870 µM (formulation) vs 8.456 µM (free drug); no carrier control was run.

5. Future perspectives

Several studies would strengthen this work. Replicate batches and storage, serum and freeze-drying stability studies are needed to show reproducibility. Release should be followed for 24–72 h under sink conditions with a free-drug control, and at pH 5.5 to mimic the tumour environment. Cell studies should include a drug-free carrier control, exposure of 72 h or longer, BRCA-mutated lines (for example MDA-MB-436 or HCC1937) alongside BRCA-proficient MDA-MB-231 cells, and a non-cancer control line. Uptake, PARP-trapping and DNA-damage (γH2AX), cell-cycle and apoptosis assays would explain the mechanism, and DSC and XRD would show the physical state of the drug in the particles. PEGylation or ligand-based targeting could improve circulation time and tumour uptake, and pharmacokinetic, biodistribution, xenograft and haematological-toxicity studies would be required before clinical translation, together with scale-up and a less toxic replacement for DMSO.

6. Conclusions

Talazoparib-loaded PDLG–lecithin L-PNPs were prepared by nanoprecipitation method and optimised with a Box–Behnken design. The optimised formulation had a particle size of about 127 nm, a PDI of 0.379, a zeta potential of −21.3 mV and 89.75 % entrapment

efficiency, with no FTIR evidence of incompatibility. The formulation showed progressive release and a lower IC_{50} than free drug in MDA-MB-231 cells, but the poor predictive power of the models and the lack of a carrier control mean that these findings are preliminary. Replicated batches, longer release and stability studies, a blank-carrier control and testing in BRCA-mutated cell lines are the next steps.

Declarations

Origin of the work: This article is derived from the M.Pharm dissertation of the first author, The Tamil Nadu Dr. M.G.R. Medical University, Chennai, supervised by the corresponding author.

Ethics: Only a commercial cell line was used; no human participants or animals.

Acknowledgements: The authors thank Corbion (Mr. Lee Chin) for providing PURASORB® PDLG 5002A, the BioMe laboratory, Karaikudi, for the *in-vitro* cytotoxicity studies, and the Department of Pharmaceutics, KMCH College of Pharmacy, Coimbatore, and Dr. N.G.P. Research and Educational Trust for the facilities provided.

References

1. Howard FM, Olopade OI. Epidemiology of triple-negative breast cancer: a review. Cancer J. 2021;27:8–16. doi:10.1097/PPO.0000000000000500
2. Schmid P, Cortes J, Dent R, McArthur H, Pusztai L, Kümmel S, et al. Overall survival with pembrolizumab in early-stage triple-negative breast cancer. N Engl J Med. 2024;391:1981–91. doi:10.1056/NEJMoa2409932
3. Bardia A, Hurvitz SA, Tolaney SM, Loirat D, Punie K, Oliveira M, et al. Sacituzumab govitecan in metastatic triple-negative breast cancer. N Engl J Med. 2021;384:1529–41. doi:10.1056/NEJMoa2028485
4. Senkus E, Delaloge S, Domchek SM, Conte P, Im SA, Xu B, et al. Olaparib efficacy in patients with germline BRCA-mutated, HER2-negative metastatic breast cancer: subgroup analyses from the phase III OlympiAD trial. Int J Cancer. 2023;153:803–14. doi:10.1002/ijc.34525
5. Shen Y, Rehman FL, Feng Y, Boshuizen J, Bajrami I, Elliott R, et al. BMN 673, a novel and highly potent PARP1/2 inhibitor for the treatment of human cancers with DNA repair deficiency. Clin Cancer Res. 2013;19:5003–15. doi:10.1158/1078-0432.CCR-13-1391
6. Morganti S, Marra A, De Angelis C, Toss A, Licata L, Giugliano F, et al. PARP inhibitors for breast cancer treatment: a review. JAMA Oncol. 2024;10:658–70. doi:10.1001/jamaoncol.2023.7322
7. Litton JK, Rugo HS, Ettl J, Hurvitz SA, Gonçalves A, Lee K-H, et al. Talazoparib in patients with advanced breast cancer and a germline BRCA mutation. N Engl J Med. 2018;379:753–63. doi:10.1056/NEJMoa1802905
8. Litton JK, Hurvitz SA, Mina LA, Rugo HS, Lee KH, Gonçalves A, et al. Talazoparib versus chemotherapy in patients with germline BRCA1/2-mutated HER2-negative advanced breast cancer: final overall survival results from the EMBRACA trial. Ann Oncol. 2020;31:1526–35. doi:10.1016/j.annonc.2020.08.2098
9. Dasgupta A, Sofias AM, Kiessling F, Lammers T. Nanoparticle delivery to tumours: from EPR and ATR mechanisms to clinical impact. Nat Rev Bioeng. 2024;2:714–6. doi:10.1038/s44222-024-00203-3
10. Mehra NK, Tekmal RR, Palakurthi S. Development and evaluation of talazoparib nanoemulsion for systemic therapy of BRCA1-mutant cancer. Anticancer Res. 2018;38:4493–503. doi:10.21873/anticanres.12753
11. Guney Eskiler G, Cecener G, Egeli U, Tunca B. Talazoparib nanoparticles for overcoming multidrug resistance in triple-negative breast cancer. J Cell Physiol. 2020;235:6230–45. doi:10.1002/jcp.29552
12. Zhang L, Chan JM, Gu FX, Rhee JW, Wang AZ, Radovic-Moreno AF, et al. Self-assembled lipid–polymer hybrid nanoparticles: a robust drug delivery platform. ACS Nano. 2008;2:1696–702. doi:10.1021/nn800275r
13. Mukherjee A, Waters AK, Kalyan P, Achrol AS, Kesari S, Yenugonda VM. Lipid–polymer hybrid nanoparticles as a next-generation drug delivery platform: state of the art, emerging technologies, and perspectives. Int J Nanomedicine. 2019;14:1937–52. doi:10.2147/IJN.S198353
14. Karati D, Mukherjee S, Prajapati B, Bose A, Paul S, Elossaily GM, et al. A review on lipid-polymer hybrid nanocarriers in cancer. J Drug Deliv Sci Technol. 2024;97:105827. doi:10.1016/j.jddst.2024.105827
15. Godara S, Lather V, Kirthanashri SV, Awasthi R, Pandita D. Lipid-PLGA hybrid nanoparticles of paclitaxel: preparation, characterization, *in vitro* and *in vivo* evaluation. Mater Sci Eng C. 2020;109:110576. doi:10.1016/j.msec.2019.110576
16. Tahir N, Madni A, Balasubramanian V, Rehman M, Correia A, Kashif PM, et al. Development and optimization of methotrexate-loaded lipid-polymer hybrid nanoparticles for controlled drug delivery applications. Int J Pharm. 2017;533:156–68. doi:10.1016/j.ijpharm.2017.09.061
17. Dave V, Yadav RB, Kushwaha K, Yadav S, Sharma S, Agrawal U. Lipid-polymer hybrid nanoparticles: development & statistical optimization of norfloxacin for topical drug delivery system. Bioact Mater. 2017;2:269–80. doi:10.1016/j.bioactmat.2017.07.002
18. Rizwanullah M, Perwez A, Mir SR, Rizvi MMA, Amin S. Exemestane encapsulated polymer-lipid hybrid nanoparticles for improved efficacy against breast cancer: optimization, *in vitro* characterization and cell culture studies. Nanotechnology. 2021;32. doi:10.1088/1361-6528/ac1098
19. International Council for Harmonisation. ICH Harmonised Tripartite Guideline: Pharmaceutical Development Q8(R2). 2009.
20. Tripathi D, Kumari J, Rathour K, Yadav P, Shukla V, Rai AK. A review on the progress of QbD

approach in nanosystems optimization: current updates and strategic applications. Lett Drug Des Discov. 2023;21:2545–66. doi:10.2174/0115701808256947231004110357

21. Birla D, Khandale N, Bashir B, Shahbaz Alam M, Vishwas S, Gupta G, et al. Application of quality by design in optimization of nanoformulations: principle, perspectives and practices. Drug Deliv Transl Res. 2025;15:798–830. doi:10.1007/s13346-024-01681-z
22. Chadha R, Bhandari S. Drug–excipient compatibility screening—role of thermoanalytical and spectroscopic techniques. J Pharm Biomed Anal. 2014;87:82–97. doi:10.1016/j.jpba.2013.06.016
23. Sharma D, Maheshwari D, Philip G, Rana R, Bhatia S, Singh M, et al. Formulation and optimization of polymeric nanoparticles for intranasal delivery of lorazepam using Box-Behnken design: *in-vitro* and *in-vivo* evaluation. Biomed Res Int. 2014;2014:156010. doi:10.1155/2014/156010
24. Higuchi T. Mechanism of sustained-action medication: theoretical analysis of rate of release of solid drugs dispersed in solid matrices. J Pharm Sci. 1963;52:1145–9. doi:10.1002/jps.2600521210
25. Ritger PL, Peppas NA. A simple equation for description of solute release I. Fickian and non-Fickian release from non-swellable devices in the form of slabs, spheres, cylinders or discs. J Control Release. 1987;5:23–36.
26. Anwer MK, Ali EA, Iqbal M, Ahmed MM, Aldawsari MF, Saqr AA, et al. Development of sustained release baricitinib loaded lipid-polymer hybrid nanoparticles with improved oral bioavailability. Molecules. 2021;27:168. doi:10.3390/molecules27010168
27. Keung MY, Wu Y, Badar F, Vadgama JV. Response of breast cancer cells to PARP inhibitors is independent of BRCA status. J Clin Med. 2020;9:940. doi:10.3390/jcm9040940
28. Pai Bellare G, Saha B, Patro BS. Targeting autophagy reverses de novo resistance in homologous recombination repair proficient breast cancers to PARP inhibition. Br J Cancer. 2021;124:1260–74. doi:10.1038/s41416-020-01238-0